Grating-frustrated coupler: a novel channel-dropping filter in single-mode optical fiber

J.-L. Archambault, P. St. J. Russell, S. Barcelos, P. Hua, and L. Reekie

Optoelectronics Research Centre, University of Southampton, Southampton SO9 5NH, UK

Received September 20, 1993

A low-insertion-loss, all-single-mode fiber, wavelength-division-multiplexing filter comprising a four-port polished coupler and a strong fiber grating is demonstrated. The device operates in a novel way by a process we call grating-frustrated directional coupling. A fiber grating, present in only one half of the coupler, frustrates the transference of power to the other half within a narrow wavelength range. The performance of a prototype device—a 1535-nm channel-dropping filter with 0.7-nm bandwidth, 70% peak transmission, and 13-dB isolation—shows great promise for wavelength-division-multiplexing and line-filtering applications.

In recent years photorefractive fiber Bragg gratings[1] have proven extremely successful as in-line reflection filters. These gratings are compact noninvasive low-loss elements with linewidths ranging from several gigahertz to a few terahertz.[2,3] Owing to their excellent properties and increasing availability they are ideal as building blocks in new types of wavelength-selective optical components. In particular, narrow-band-transmission and wavelength-division-multiplexing filters recently were proposed[4] or demonstrated[5,6] by a combination of gratings with other optical elements such as a coupler,[4] a Mach–Zehnder interferometer,[5] and a circulator.[6] Here, for the first time to our knowledge, we analyze and demonstrate a narrow-band channel-dropping filter, consisting of a Bragg grating inscribed in one side of an evanescent field coupler, in a configuration particularly well suited to fiber geometry. The operating principle of this filter is different altogether from that of previous devices; the strong grating frustrates the transfer of power over a narrow range of wavelengths, resulting in a new type of device—the grating-frustrated coupler. As this device is all fiber and noninterferometric, in contrast with those of Refs. 5 and 6, it has the advantages of being inherently low loss and stable and potentially low cost.

Figure 1 is a schematic of the grating-frustrated coupler. Two single-mode fibers, 1 and 2, form a 2×2 directional coupler. The two fiber cores are identical, except that core 2 contains a photorefractive Bragg grating, which consists of an index modulation of period Λ and amplitude δn. The spatially averaged refractive index inside the grating, n_{av}, is equal to the index of core 1. The Bragg wavelength of the grating is given by $\lambda_B = 2n_{eff}\Lambda$, where n_{eff} is the mode index. Away from this wavelength, light propagates in the grating region as if it were in a medium of uniform refractive index n_{av}; the device is then equivalent to a synchronous coupler, able to perform a complete transfer of power between the two fibers.

Near the Bragg wavelength, within the spectral region known as the stop band, the grating has two effects: first, it introduces a strong dispersion, making the coupler asynchronous or phase mismatched; second, it creates a barrier (a one-dimensional photonic band gap) that rejects photons attempting to tunnel through. If the grating is sufficiently strong, the two effects can efficiently frustrate the transfer of optical power from one fiber to the other. With proper design parameters, a grating-frustrated directional coupler can be used as an all-fiber channel-dropping filter, transmitting wavelengths within the grating stop band through fiber 1 while other wavelengths pass through fiber 2.

Coupled-wave theory was used to model this grating-frustrated coupler by use of an approach similar to that for grating-assisted couplers.[7] In the analysis, light propagating in each of the two fibers is decomposed into a backward and a forward guided wave. In the coupling region, which has an effective length L_C,[8] each pair of copropagating waves exchanges power with a coupling constant C; inside the grating region of length L_G the forward and the backward waves of fiber 2 are also coupled together, with a coupling constant $\kappa = \pi\delta n/\lambda$, where λ is the vacuum wavelength. If the coefficients C and κ are assumed constant over the coupler and grating regions, respectively, then we can calculate analytically the fraction of the input power at each of the four output ports (T_1, T_2, R_1, and R_2) by solving four coupled-wave equations.

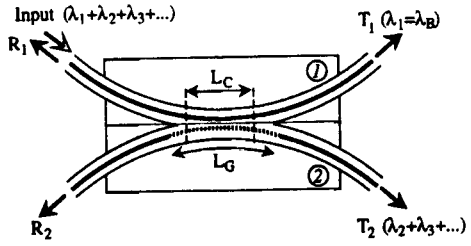

Fig. 1. Schematic of a grating-frustrated coupler, comprising two fibers, 1 and 2, in a coupler configuration (L_C is the effective coupler length). Fiber 2 contains a Bragg grating of length L_G.

0146-9592/94/030180-03$6.00/0

For a nearly complete exchange of power to occur between the two fibers outside the grating bandwidth, the product CL_C must be equal to a half-multiple of π at the wavelength of operation. For the grating to be effective at frustrating coupling, our calculations show that the coupling constant C must be small in comparison with the grating coupling constant κ; it is therefore preferable to choose the smallest value of C, given by $CL_C = \pi/2$. Figures 2(a) and 2(b) show how the four outputs of a grating-frustrated coupler vary with the grating strength at the Bragg wavelength. For $\kappa = 0$ the device is a conventional 2×2 coupler, and since $CL_C = \pi/2$ there is a complete transfer of power, with $T_2 = 100\%$. As the grating strength is increased, however, T_2 decreases to zero, and T_1 tends to 100%. A large fraction of the input light can also be reflected, as seen in Fig. 2(b). For $L_G = L_C$ the reflected signals peak at $\kappa L_C \sim 2$ but then decay to zero for larger values of κL_C. It is clear that the stronger the grating is, the more effective it is at frustrating coupling at the Bragg wavelength. Figure 2 also shows the effect of extending the grating beyond the coupling region. The longer the grating, the more difficult it is for light to escape through either end of fiber 2, and therefore an important decrease is observed in T_2 and R_2 when the grating length is increased from L_C to $2L_C$. Consequently, a larger fraction of power is found in the output ports of fiber 1, with R_1 being favored in weaker gratings and T_1 in stronger ones.

In our calculations we have observed that the bandwidth of the grating-frustrated coupler is given to a good approximation by the bandwidth of the grating alone. As an example, we show in Fig. 3 the calculated reflection and transmission spectra near the Bragg wavelength of a grating-frustrated coupler with $\kappa L_C \sim 3$ and $L_G \sim 2L_C$. The FWHM bandwidth of the transmission spectrum T_1 is $\Delta\lambda \sim 0.7$ nm, very close to that of a grating with the same index modulation and length. This spectrum has characteristic central dip because the phase mismatch caused by the grating actually reaches a maximum at the edges of the grating stop band, which are located at $\lambda = \lambda_B(1 \pm \delta n/2n_{\text{eff}})$.

The various parameters must be chosen carefully for the grating-frustrated coupler to work as a useful filter. In general T_1 should be maximized and T_2, R_1, and R_2 should be minimized at the Bragg wavelength. Also, for many (though not all) applications, one would like the filter bandwidth to be as small as possible. We can meet the first requirement by making κL_C as large as possible and can achieve this by having either a large index modulation or a long coupler region. However, the index modulation is limited not only by photorefractivity of fiber 2 but also by the desired filter bandwidth, since $\Delta\lambda \sim \delta n \lambda_B / n_{\text{eff}}$ for a strong grating. Increasing the coupler length also has its limitations; the longer a coupler is, the more difficult it is to obtain a complete exchange of power inside the coupler. In practice the average indices of the two fibers forming the coupler will always be mismatched by a small amount, Δn_{av}; for $CL_C = \pi/2$, the maximum power transfer achievable by the coupler (outside the grating bandwidth) is then limited to[9]

$$P = \frac{1}{1 + (2\Delta n_{\text{av}} L_C/\lambda)^2}, \tag{1}$$

which decreases quadratically with L_C if P is close to 100%.

Taking into account these various considerations in the choice of parameters, we fabricated a grating-frustrated coupler by incorporating a photorefractive fiber grating into one half of a polished fiber coupler.[8] Before making the coupler we wrote a grating with $\lambda_B = 1535$ nm and $\Delta\lambda = 1.1$ nm in fiber 2, by exposing from the side a germania/boron-codoped optical fiber over a 15-mm length for ~10 min to two interfering UV beams from a KrF excimer laser. This resulted in an index modulation of $\delta n \sim 6 \times 10^{-4}$ and also raised the average index of the fiber by $(8.7 \pm 0.3) \times 10^{-4}$, which we estimated by carefully monitoring the change in Bragg wavelength during the exposure. In order to ensure that the average indices of the two fibers would be matched to within $\Delta n_{\text{av}} \sim 6 \times 10^{-5}$, a similar grating was also written in fiber 1, but at $\lambda_B = 1550$ nm. The 15-nm spacing between the Bragg wavelengths was large enough to permit the two gratings to be treated independently of each other. (One could avoid having to write two gratings to match the average fiber indices, simply by choosing two initially dissimilar fibers and writing a grating only in the fiber with the lower mode index

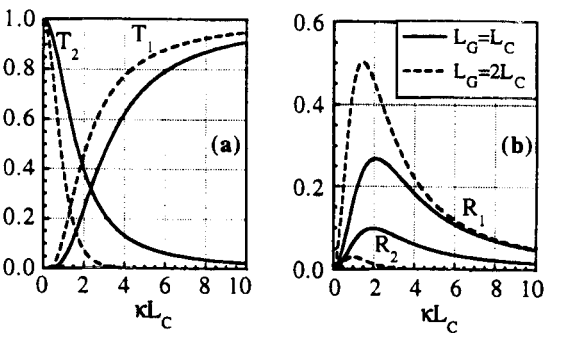

Fig. 2. Dependence of the four outputs on grating strength at the Bragg wavelength and for two grating lengths for (a) transmission and (b) reflection.

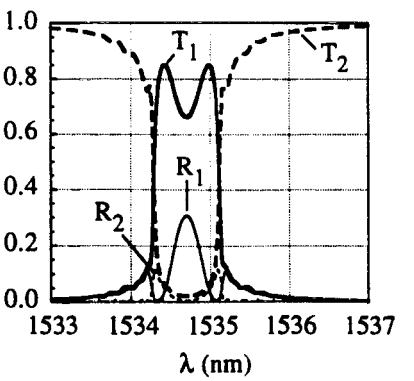

Fig. 3. Calculated reflection and transmission spectra for $L_C = 2.5$ mm, $L_G = 4.5$ mm, $n_{\text{av}} = 1.45$, $\delta n = 6 \times 10^{-4}$, and $\lambda_B = 1534.7$ nm.

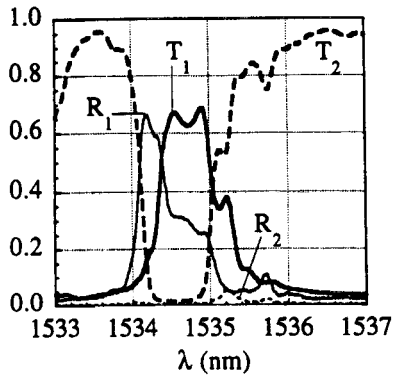

Fig. 4. Measured reflection and transmission spectra of an all-fiber grating-frustrated coupler.

of the two.) After these exposures we fabricated a coupler by mounting each fiber into a glass block and polishing it to within 2 μm of the core, following the method described in Ref. 8. The two blocks were assembled in a precision jig for submicrometer control of the fiber alignment. The radius of curvature of the fibers in the blocks was chosen to give an effective coupling length of $L_C \sim 3$ mm, corresponding to $\kappa L_C \sim 3.7$. According to Eq. (1) and with the assumption that $\Delta n_{av} \sim 6 \times 10^{-5}$, this 3-mm length should permit at least 95% coupling.

Light from a broadband 1540-nm light-emitting diode was launched into fiber 1, and the coupler was tuned until output T_2 was maximized. A maximum coupling of 97% was thus obtained, indicating an average index mismatch of $\Delta n_{av} \sim 5 \times 10^{-5}$, which is within the error predicted. The wavelength response of the coupler was examined by use of a white-light source and optical spectrum analyzer. The coupling was seen to decrease by only 1% over a 100-nm wavelength range centered at 1535 nm. A cutback measurement was also performed to compare the total amount of power form all four outputs with the input power launched in fiber 1; the excess loss of the coupler was found to be ~0.22 dB, which is comparable with previously reported values.[8] The device was further characterized by the introduction of a 50:50 fiber coupler between the light-emitting diode and the input port in order to have access to output R_1. The calibrated reflection and transmission spectra measured at the four ports are shown in Fig. 4. Output T_1 has a maximum of ~70% and a bandwidth of 0.7 nm, which is smaller than the original grating bandwidth. The spectrum has the characteristic central dip predicted from our calculations. Away from the Bragg wavelength ($\lambda_B = 1534.7$ nm) the transmission drops to $T_1 \sim 3\%$, corresponding to a 13-dB extinction ratio. The other transmission spectrum, T_2, has a 1.0-nm bandwidth and 18-dB extinction (1.6% transmission) at the Bragg wavelength. The dip in transmission at 1533 nm is due to resonant coupling into a cladding mode. The reflected signal R_1 is larger than expected, with a prominent feature at 1534.2 nm, whereas R_2 remains small at all wavelengths, with a 5% maximum at 1535.2 nm.

In Fig. 3 a good theoretical fit of the measured spectra was obtained for $L_C = 2.5$ mm, $L_G = 5$ mm, and $\delta n = 6 \times 10^{-4}$. The discrepancies that can be observed are due mainly to the nonuniformity of the index modulation and the average index along the grating region, caused by spatial intensity variations in the UV writing beam. The reflection peak at 1534.2 nm probably originates from an underexposed grating section located outside the coupler region. This would also explain why the main peak in the T_1 spectrum is narrower than the dip in the T_2 spectrum.

In summary, a useful all-fiber channel-dropping filter has been designed and demonstrated by a combination of two established technologies: the polished fiber coupler and photorefractive fiber gratings. The grating-frustrated coupler operates on the principle that, over a narrow range of wavelengths corresponding to the grating stop band, coupling is prevented by a strong grating that detunes the coupler and creates a one-dimensional photonic band gap. Coupled-wave theory has provided an accurate description of the properties of grating-frustrated couplers, permitting us to establish practical limits in the choice of parameters and to optimize the design. Our first prototype, operating at 1535 nm, has already produced excellent results—0.7-nm bandwidth, 13-dB isolation, 70% peak transmission, and 0.22-dB excess loss—and better performance is to be expected in the future. The critical steps in improving the device performance would be to use a more uniform grating and to reduce the index mismatch between the two fibers. Both improvements would help increase the isolation of the transmitted signals while reducing the reflected signals and the bandwidth of the device. The grating-frustrated coupler could also be designed for planar geometry.

References

1. G. Meltz, W. W. Morey, and W. H. Glenn, Opt. Lett. **14,** 823 (1989).
2. J.-L. Archambault, L. Reekie, and P. St. J. Russell, Electron. Lett. **29,** 28 (1992).
3. P. J. Lemaire, R. M. Atkins, V. Mizrahi, and W. A. Reed, Electron. Lett. **29,** 1191 (1993).
4. H. A. Haus and Y. Lai, J. Lightwave Technol. **10,** 57 (1992).
5. R. Kashyap, G. D. Maxwell, and B. J. Ainslie, IEEE Photon. Technol. Lett. **5,** 191 (1993).
6. D. R. Huber, in *Eighteenth European Conference on Optical Communication* (VDE-Verlag, Berlin, 1992), paper We P2.2.
7. D. Marcuse, *Theory of Dielectric Optical Waveguides,* 2nd ed. (Academic, London, 1991), Chap. 7, pp. 280–293.
8. M. J. F. Digonnet and H. J. Shaw, IEEE J. Quantum Electron. **QE-18,** 746 (1982).
9. A. W. Snyder and J. D. Love, *Optical Waveguide Theory* (Chapman & Hall, London, 1983), Chap. 18, p. 399.